ENERGY AND WATER MANAGEMENT IN PHOTOVOLTAIC AND MOF-303-BASED HYBRID SYSTEMS

by

Selda GOZUBUYUK[a,b*], Gokhan OMEROGLU[b], and Ahmet Numan OZAKIN[b]

[a] Department of Motor Vehicles and Transportation Technologies, Technical Sciences Vocational School, Bingol University, Bingol, Turkiye
[b] Department of Mechanic Engineering, Faculty of Engineering, Ataturk University, Erzurum, Turkiye

Original scientific paper
https://doi.org/10.2298/TSCI2504187G

Metal-organic frameworks (MOF), as an innovative material, have been tested in various systems and devices for water production. However, no studies have been encountered regarding water production using hot air generated by photovoltaic systems. In this study, the effect of air heated via photovoltaic panels on water production was investigated by delivering it to the surface of MOF material. Different irradiation levels (900 W/m², 1000 W/m², and 1100 W/m²), fan speeds (1.0 m/s, 1.6 m/s), MOF quantities (100 g, 200 g), and MOF box dimensions (0.06190 m², 0.07712 m²) were tested. According to the results, for each irradiation level, the thickness of the MOF-303 material increased when the surface area was reduced, leading to an extended water extraction duration. Additionally, it was observed that higher air velocities resulted in a longer water extraction time. This phenomenon is attributed to the reduction in the temperature of the air delivered to the MOF-303 surface at higher air velocities, which is initially heated via the photovoltaic panel. Consequently, the water production duration increased. Based on the experimental data, the amount of water produced ranged between 0.30 mL and 1.17 mL.

Key words: *solar energy, harvesting of water, MOF-303, PV*

Introduction

Water, an invaluable resource for existence and continuity, holds undeniable importance not only for humans but also for other living organisms, ecosystems, and habitats. The natural atmosphere contains approximately 13 sextillion liters of water [1]. Of the Earth's water, 97.2% is stored in the oceans, while the remaining portion exists as water vapor in the atmosphere, or in lakes, rivers, and glaciers. However, freshwater is essential for sustaining life. Freshwater constitutes only 2.5% (10633450 km³) of the Earth's water. Global water consumption continues to increase steadily. Furthermore, climate change caused by global warming, the increased frequency of extreme weather events, and the pollution of clean water sources are depleting the availability of clean freshwater resources [2]. As a result, it is anticipated that by 2050, 50% of the world's population will face water scarcity due to the contamination of surface waters and the depletion of underground reservoirs [3]. While various water production techniques are employed to address this issue, in recent years, MOF have emerged as promising materials for water harvesting. Their unique characteristics, including porosity, high specific

* Corresponding author, e-mail: sgozubuyuk@bingol.edu.tr

surface areas, ideal isotherm profiles, absorption and desorption capabilities, and water-binding properties, make them highly suitable for this purpose [4].

The MOF are a class of porous polymeric materials composed of metal ions interconnected by bridging ligands [5]. The MOF have emerged as a highly promising material class with numerous applications, including gas storage (*e.g.*, methane and hydrogen), high capacity adsorbents, thin-film devices, biomedical applications, catalysts for separation processes, and water production. However, not every reported MOF type is suitable for all applications. Consequently, their utility varies over time, depending on their structural properties and specific application requirements.

Laha *et al.* [6] a nanocomposite material obtained by blending graphene, aminokil, and CuBTC MOF was found to have a 39.5% higher water uptake capacity and a 69.2% higher maximum water efficiency compared to the conventional CuBTC MOF material. Additionally, the nanocomposite material demonstrated a daily maximum water production of 0.445 g/g. Sharma *et al.* [7] an innovative composite material was created by combining MOF 808 with alginate via ionic gel polymerization. This composite exhibited a high water uptake capacity (∼1.02 g/g, 75% RH, 25 °C) and high water release capacity due to the presence of Fe_3O_4. Hanikel *et al.* [8] it was reported that the MOF-LA2-1 material synthesized using a binding strategy provided a 50% increase in moisture retention capacity compared to MOF-303. Luo *et al.* [9] the hybridization of MIL-160 with MOF-303 resulted in a significant increase in both specific surface area and pore volume, and the resulting hybrid material was reported to exhibit high moisture retention capacity under relative humidity conditions of 30% and below (RH ≤ 30) (0.44 g/g). Bilal *et al.* [10] the effects of different MOF types on water production at various temperatures and relative humidity levels were evaluated. Chen *et al.* [11] the performance of CAU-10-H, MOF-303, and Ni_2Cl_2 (BTDD) materials in powder form was compared with their block-form counterparts under specific pressure conditions. The results revealed that the water absorption capacity of MOF materials used in block form decreased by approximately 50%, and the moisture absorption time significantly increased. Zheng *et al.* [12] derivatives of MOF-303 were created by adding varying amounts of TDC-2 (thiophene-2,5-dicarboxylate) to MOF-303, enabling the adjustment of the material's hydrophilicity. Luo *et al.* [13] designed a solar-triggered monolithic adsorbent by combining polyaniline/chitosan layers with a glass fiber support, resulting in the creation of a BMOF material. The designed monolithic adsorbent produced 1.19 g of water daily. Almassad *et al.* [14] the water production amounts of the best water collection devices were compared, and the results showed that the designed device achieved a 169% increase in water production. Wu *et al.* [15] three carbon-based materials – CNT (carbon nanotubes), G (graphite), and CB (carbon black powder) – were combined with MOF-801 in a 67:33 ratio to form three composite adsorbents: MOF-801/CNT, MOF-801/G, and MOF-801/CB. The best-performing composite was found to be MOF-801/CNT.

Table 1 provides a comprehensive review of water production capacities of various MOF types under different operating conditions reported in the literature. Tao *et al.* [16] reported that a volumetric MOF monolith (CAS) was obtained by placing well-aligned Al-Fumarate MOF rods on a carbon scaffold (CS) with a porous structure. The resulting material produced approximately 1.95 L/kg of water daily. Li *et al.* [17] demonstrated that the MIL-101 (Cr) material facilitated fast moisture diffusion and vapor release via open channels, resulting in a daily water production of 15.9 L/kg. According to the study of Logan *et al.* [18] the effects of thickness, temperature, and relative humidity on water production were examined for nine different MOF types, including Zn-ZIF-8, Al-MIL-53, Cu-HKUST-1, Ti-MIL-125, Zr-UiO-66, Ti-MIL-125-NH2, Cr-MIL-101, Zr-MOF-808, and Zr-UiO-66-NH2. Fuchs *et al.* [19] used Ra-

Table 1. Literature review: water production capacities of various MOF types under different operating conditions [20-28]

Publication	Working conditions	MOF	Amount of water produced
[20]	25 °C RH = %30	$CaCl_2$ at MOF-808-11.8	1.8 kg/kg
[21]	25 °C RH = %20	MXene Ti_3C_2 at UiO-66-NH_2	57.8 ml/kg
[22]	35°C desorption	Ni-IRMOF74-III	0.18 kg/kg
[23]	25 °C RH = %20 RH = %35 RH = %60	PCS at MOF tube-shaped membrane	6.2 L/kg 3.2 L/kg 8.6 L/kg
[24]	25 °C RH = %60	MOF at ACF-LiCl	2.2 g/g
[25]	25 °C RH = %90	UIO-66-NH_2	Time: 10 h 1.9 g/g
[26]	25 °C and RH = %60 RH = %70 RH = %90	MIL-101(Cr) (M) MIL-101(Cr)/ $CaCl_2$ (MS) MIL-101(Cr)/GO (MG) and MIL101(Cr)/GO/$CaCl_2$ (MGS)	M: 0.74,0.81,0.84 g/g MS: 0.48,0.52,0.68 g/g MG: 0.79,0.88,0.93 g/g MGS:0.63,0.69,1.08 g/g
[27]	RH = %20	MOF-801[Zr6O4$(OH)_4$(fumarate)$_6$	2.8 L/kg
[28]	22 °C RH = %18 (per day 40 cycles) 23.5 °C RH=%39 (per day 55 cycles)	MOF-801	0.33 L/h/kg 0.52 L/h/kg
[8]	27 °C RH = %32 (indoor area) 27 °C RH = %10 (in conditions Mojave desert)	MOF-303	1.3 L/kg.day 0.7 L/kg.day

man spectroscopy to enhance the water uptake capacity of single-crystal MOF-801 by 20 times through light-material interaction. As a result, the daily water production was found to be 91.9 L/kg. Kim *et al.* [29] observed that a device designed using MOF-801[Zr6$O_4$$(OH)_4$(fumarate)6] material achieved over 0.25 L/kg of water production daily under conditions with 10%-40% relative humidity. In the study of Vanleuven *et al.* [30] a neutral (zwitterionic) MOF (Ni-ZW-MOF) was used in multiple cycles under varying humidity levels, producing 126 ml/kg of water per cycle daily. Hanikel *et al.* [31] showed that employed X-ray diffraction and density functional theory calculations to analyze the water uptake model of MOF-303 material. The MOF crystals were surface-coated with uniform liquid metal nanoparticles using a laser shock evaporation technique, allowing the MOF material to accumulate on the surface. This method was anticipated to increase the thermal conductivity by up to five times compared to pure MOF and accelerate the water desorption process [32]. Feng *et al.* [33] determined that a MOF-based water collector with cooling-assisted sorption-desorption properties was designed. The system

demonstrated extraordinary productivity, producing 7.75-22.81 L H_2O/kg MOF/day under various climate conditions (10-35 °C, 20-80% RH). Additionally, with the integration of a heat pump, it achieved a productivity of 9.9 L H_2O/kg MOF/day with an energy consumption of 2.96 kW. A new hydrophilic hybrid MOF composed of MIL-160(Al) and MOF-303 was developed in another study. The obtained material exhibited improved moisture retention capacity, particularly in dry environments, and enabled the production of 0.94 g of water daily using a designed monolithic adsorbent [34]. Torres-Herrera *et al.* [35] revealed that a rectangular prism-shaped adsorbent bed was immersed in low humidity air at a specific angle, resulting in adsorption from the cooler surface of the adsorbent and creating a density parallel to the surface. This approach aimed to eliminate the discontinuity of water adsorption and desorption cycles. Kim *et al.* [36] conducted energy and exergy analyses for MOF-303 and MOF-801 materials using adsorption-based water collection technologies. Lassitter *et al.* [37] stated that a multivariate MOF material was obtained by integrating 50/50 organic binders with MOF-303 and MOF-333, which enabled the adjustment of diffusion speed – a feature not easily achievable with conventional adsorbent materials. Furthermore, a MOF-coated tube was developed to investigate the effects of diffusion parameters on water collection mechanisms. Wu *et al.* [21] presented that MOF material was coated on Ti_3C_2/sHBP using a spray method, and the resulting TCM were equipped with both solar energy and electric heating systems. When sufficient sunlight was available, solar-based air-water-harvesting (AWH) was used, and in the absence of sunlight, electric heating-based AWH was preferred. This approach aimed to achieve excellent water efficiency with significantly reduced energy costs.

A detailed review of the literature reveals that various types of MOF materials have been utilized for water production purposes. Additionally, numerous device and system designs have been proposed. However, there has been no research related to water production through the use of hot air generated by photovoltaic (PV) systems, specifically via PV/T systems. The present study introduces an innovative approach to systems designed for water production. What makes the proposed system unique is the production of water from MOF-303 material using air-based cooling, which is employed to cool the PV panel (in order to prevent the decrease in electrical efficiency caused by temperature rise). Furthermore, the study investigates the effects of heat provided by varying radiation levels and fan speeds, along with different MOF quantities and surface areas of the MOF container. The results of the tests reveal the impact of environmental temperature, the thickness of the MOF material, and the temperature reaching the top surface of the MOF material on water production.

Materials and methods

Experimental system

An experimental system has been developed to identify the factors affecting the water desorption capacity of MOF-303 material. With the developed system, tests were conducted under different radiation levels (900 W/m², 1000 W/m², and 1100 W/m²), fan speeds (1.0 m/s, 1.6 m/s), MOF quantities (100 g, 200 g), and different MOF box sizes (0.0619 m², 0.07712 m²).

Different MOF boxes of experimental process were given in fig. 1. The panel dimensions were chosen 0.357 m × 0.424 m. A control volume was created at the bottom of the panel, and a fan was placed inside this volume to transfer the heated air on the surface of the MOF-303 material. Through this set-up, the water desorption capacity of the MOF-303 material, influenced by the heat transferred to its surface, was investigated. Additionally, the fan placed in the control volume beneath the panel facilitated cooling of the panel, allowing for the evaluation of the impact of cooling on panel efficiency.

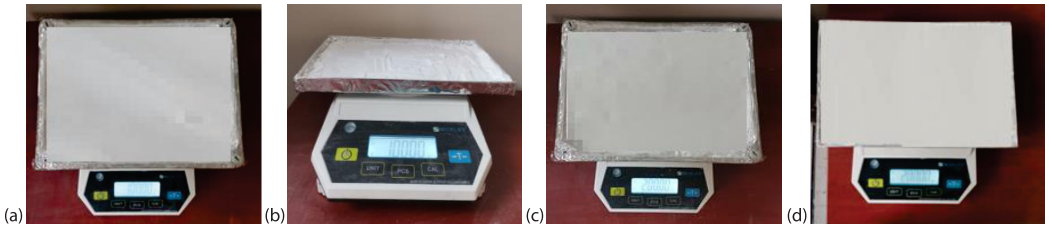

Figure 1. Different MOF boxes; (a) 100 g 1st box, (b) 100 g 2nd box, (c) 200 g 1st box, and (d) 200 g 2nd box

Since it is not possible to maintain constant conditions when using direct sunlight, six halogen projectors were employed. The irradiance intensity reaching the panel was adjusted using a Hukselfux SR05-DA2 model pyranometer, and different irradiance values were experimentally adjusted with a VARSAN-Varyak voltage regulator. Moreover, the fan speed used to transfer the heated air to the MOF-303 surface was measured with a Testo Anemometer. A thermocouple was used to determine the inlet and outlet air temperatures, the surface temperature of the PV panel, the temperatures of the top and bottom surfaces of the MOF material, and the temperatures inside the generated hot air chamber. The collected data was recorded in real time using a NOVUS Field Logger.

The image and schematic diagram of the experimental system were given in fig. 2. In the experimental system, after the irradiance intensity was adjusted using the pyranometer, the heated air was transferred to the surface of the MOF-303 material via a fan, activating the moisture desorption capacity of the MOF material. The system was operated until it reached stability.

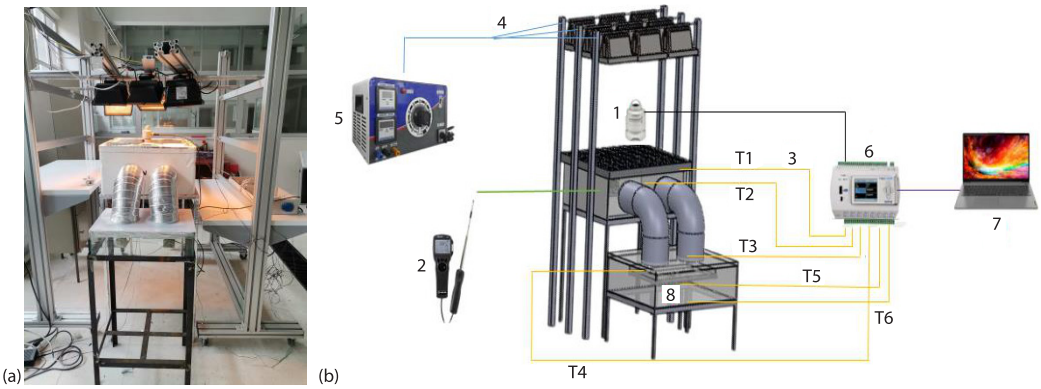

Figure 2. (a) Experimental system and (b) schematic diagram of the experimental system: *1 – pyranometer, 2 – anemometer, 3 – thermocouple, 4 – halogen projector, 5 – variac, 6 – data logger, 7 – computer, and 8 – MOF-303*

A total of 24 experiments were conducted in the designed experimental system for three different irradiance intensities, two different fan speeds, two different MOF material box sizes, and two different MOF quantities.

As it was seen in tab. 2, the water collection capacity of a specific MOF structure was tested by exposing it to different radiation intensities. At a radiation intensity of 900 W/m², 3.18 mL of water was collected, at 1000 W/m², 4.31 mL, and at 1100 W/m², 6.58 mL of water was collected. These results indicate that the water collection capacity of the MOF increases with higher radiation intensity. Additionally, key parameters influencing water production efficiency include the amount of MOF used, the surface area of the MOF container, and the air-

flow speed used to heat the MOF surface. The most significant parameters determining water production efficiency are, in order, the amount of MOF, the air-flow speed, and the surface area of the container; among these parameters, the amount of MOF has the most decisive effect on water collection capacity.

Table 2. Experimental design: MOF box size, irradiation intensity, air velocity, and MOF quantity

Experiment number	Irradiance	Fan speed	MOF amount	MOF box size	Water collected in each experiment
1	900 W/m^2	1.6 m/sn	100 g	0.07712 m^2	0.30 mL
2	1000 W/m^2	1.6 m/sn	100 g	0.07712 m^2	0.50 mL
3	1100 W/m^2	1.6 m/sn	100 g	0.07712 m^2	0.82 mL
4	900 W/m^2	1.6 m/sn	100 g	0.0619 m^2	0.32 mL
5	1000 W/m^2	1.6 m/sn	100g	0.0619 m^2	0.48 mL
6	1100 W/m^2	1.6 m/sn	100 g	0.0619 m^2	0.64 mL
7	900 W/m^2	1.6 m/sn	200 g	0.07712 m^2	0.48 mL
8	1000 W/m^2	1.6 m/sn	200 g	0.07712 m^2	0.64 mL
9	1100 W/m^2	1.6 m/sn	200 g	0.07712 m^2	1.00 mL
10	900 W/m^2	1.6 m/sn	200 g	0.0619 m^2	0.50 mL
11	1000 W/m^2	1.6 m/sn	200 g	0.0619 m^2	0.70 mL
12	1100 W/m^2	1.6 m/sn	200 g	0.0619 m^2	1.17 mL
13	900 W/m^2	1.0 m/sn	100 g	0.07712 m^2	0.45 mL
14	1000 W/m^2	1.0 m/sn	100 g	0.07712 m^2	0.45 mL
15	1100 W/m^2	1.0 m/sn	100 g	0.07712 m^2	0.75 mL
16	900 W/m^2	1.0 m/sn	100 g	0.0619 m^2	0.38 mL
17	1000 W/m^2	1.0 m/sn	100 g	0.0619 m^2	0.50 mL
18	1100 W/m^2	1.0 m/sn	100 g	0.0619 m^2	0.76 mL
19	900 W/m^2	1.0 m/sn	200 g	0.07712 m^2	0.40 mL
20	1000 W/m^2	1.0 m/sn	200 g	0.07712 m^2	0.54 mL
21	1100 W/m^2	1.0 m/sn	200 g	0.07712 m^2	0.84 mL
22	900 W/m^2	1.0 m/sn	200 g	0.0619 m^2	0.35 mL
23	1000 W/m^2	1.0 m/sn	200 g	0.0619 m^2	0.50 mL
24	1100 W/m^2	1.0 m/sn	200 g	0.0619 m^2	0.60 mL

Mathematical formulation

The efficiency of a PV cell refers to the portion of solar energy that can be converted into electricity through the PV effect. The power provided by the panel is given:

$$P_{\text{cikis}} = P_N \frac{G}{G_{\text{ref}}}\left[1 + K_T\left(T_y - T_{\text{ref}}\right)\right]$$

where P_N is the power of the panel under standard conditions, G – the incoming solar irradiance, G_{ref} – the solar irradiance under standard conditions (G_{ref} = 1000 W/m^2), K_T – the temperature

coefficient for maximum power (for polycrystalline silicon panels $K_T = 3.7 \cdot 10^{-31}$ 1/°C), T_y – the surface temperature of the panel, and T_{ref} – the reference temperature of the panel under standard conditions ($T_{\text{ref}} = 25$ °C) (and P_{cikis} is the output power of the panel.

$$\eta = \frac{P_{\text{cikis}}}{GA}$$

The area of the panel is represented by A, while η represents the efficiency of the panel [38].

Research findings

The water production cycle occurs in two main stages:

- *Capture cycle*: In this stage, the functions of easy water uptake and release are performed.
- *Collection cycle*: In this stage, cooling energy is provided to allow the condensation of the released water vapor, ensuring that the condensation temperature is set lower than the temperature of the released water vapor.

In the first stage of the water production cycle, known as the capture cycle, the unsaturated MOF begins to reach its saturation point. After this point, thermal processes such as sunlight, warm air, or halogen projectors are applied to release the captured water from the MOF. In the collection cycle, the released water vapor increases the humidity of the air surrounding the MOF, and this process continues throughout the day. When the hot and humid air is cooled to the dew point by ambient cooling techniques, condensation occurs, and the vapor phase of water transitions to the liquid phase, completing the water production process [4].

When fig. 3 is examined, the MOF-303 material is exposed to ambient air for a minimum of two hours and up to a maximum of 12 hours depending on humidity levels, in order to absorb moisture. This process is typically carried out during the nighttime. The primary reason for this is that the lower nighttime temperatures result in higher relative humidity, which increases the moisture absorption capacity of MOF-303. After the moisture collection process is completed, the material needs to be heated to release the absorbed moisture. In the study conducted for this purpose, a control volume was placed beneath the PV panel. The airflow provided by the fan in the control volume allowed the air to heat up through the panel. The heated air then heated the surface of the MOF-303, enabling the release of moisture. Initially, the moisture is released in the vapor phase, and as the temperature difference increases, condensation occurs. Over time, the vapor will turn into droplets, and these droplets will merge to form liquid water.

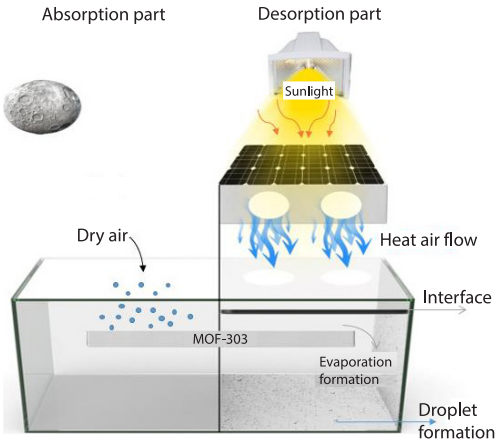

Figure 3. Water release mechanism

When water molecules reach sufficient energy, the water molecules inside the pores move outward due to intermolecular repulsive forces in the evaporation formation stage. Once the water molecules exit the pores, they spread across the surface of the environment where the MOF container is placed as free water vapor. At this stage, the water molecules are no longer bound to the MOF and are in the gas phase.

After the experimental system is started, evaporation occurs on the surfaces of the insulated control volumes created for evaporation purposes in all experiments, generally within a time interval of 15-30 minutes, as shown in fig. 4(a).

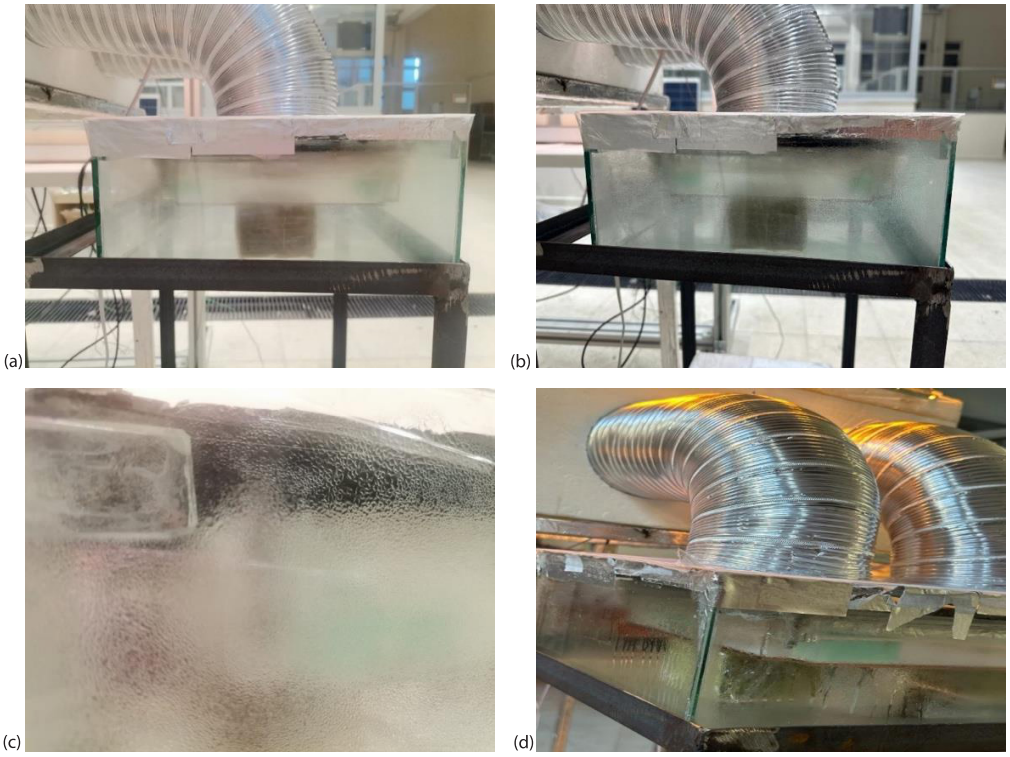

Figure 4. The stages of the experimental system;
(a) evaporation observed in the experimental system, (b) formation of droplets,
(c) growth of droplets, and (d) water formation

When vapor molecules condense on a cold surface, microscopic roughness or particles on the surface act as centers for droplet nucleation in the droplet formation stage. According to fig. 4(b), in the experimental system, after evaporation, an increase in surface temperature and the ambient air reaching condensation temperatures will trigger droplet formation. The small droplets formed on the surface can merge to form larger droplets. This merging accelerates the growth of water droplets on the surface. Figure 4(c) shows that once droplet formation begins, the droplets will grow as the difference between the ambient air and the surface temperature increases.

As the droplets grow and gain mass, they move across the surface. Under the influence of gravity, they flow along the slope of the condensing surface. As seen in fig. 4(d), after the droplets have grown, water formation occurs as the droplets merge together.

When the experimental results obtained under 900 W/m² irradiation are evaluated, it is observed, as shown in fig. 5, that the water production time increases with the increasing amount of MOF-303 placed in the MOF box with a surface area of 0.06190 m². Thus, it is predicted that the material thickness increases in direct proportion the time [39]. The main reason for the observed changes in water production time as the MOF thickness increases is the diffusion rate of water molecules in the gas phase throughout the material. In a thick

MOF layer, the penetration of water molecules into the material and their reach to the internal pores takes longer. This is directly related to the diffusion rate. According to Fick's law of diffusion, there is a non-linear relationship between the diffusion time and the distance traveled [40]. That is, as the thickness increases, it takes more time for gas molecules to travel through the material. Particularly, the high internal surface area and organized pore structures of MOF lead to a large portion of the adsorption area for these molecules being located in the internal layers of the material. Therefore, as the thickness increases, the time required for the gas-phase molecules to reach all the adsorption areas also increases. Additionally, based on experimental data, the amount of water produced under 900 W/m² irradiation ranged between 0.3 mL and 0.5 mL.

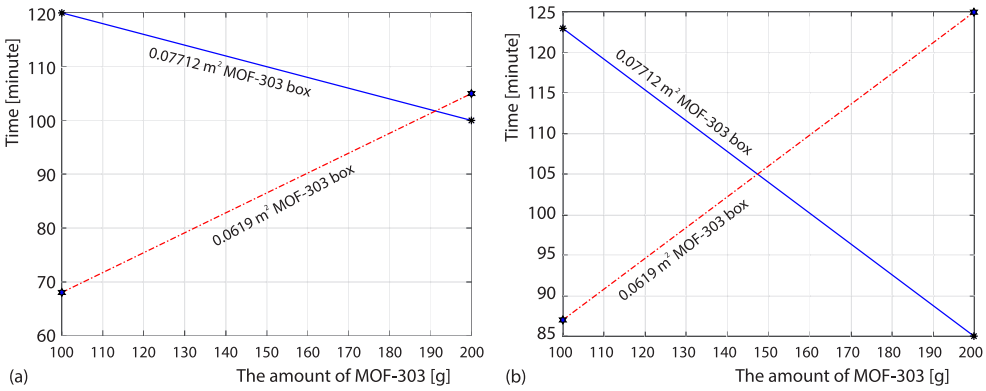

Figure 5. Water production in MOF boxes with different surface areas using different amounts of MOF-303 under 900 W/m² irradiation; (a) 1.0 m/s air speed and (b) 1.6 m/s air speed

The experimental studies conducted under 1000 W/m² irradiation yielded water amounts ranging from 0.45-0.70 mL. Among the experiments, the shortest water production time was observed under conditions of 1000 W/m² irradiation, 100 g of MOF, and 1.0 m/s air speed.

When examining the results of the experiments in fig. 6, it is evident that as the thickness of the box with a surface area of 0.07712 m² increases, the water production time decreases. The reason for this is that thicker MOF structures improve the accessibility of internal pores. This allows water molecules to move more quickly within the pores, thereby shortening the water production time. Additionally, the increased thickness of the material in the box helps reduce the time required for water production due to various factors. One of these factors is heat distribution. A thick MOF facilitates more uniform heat distribution, minimizing temperature fluctuations during the adsorption process. Furthermore, the thicker structures support more effective interaction between the air-flow, water vapor, and the MOF surface, thereby accelerating water production. The combination of all these factors highlights the efficiency gains provided by MOF with larger surface areas and thicker structures in water production processes, significantly reducing the time required to collect water.

Under 1100 W/m² irradiation, the amount of water obtained ranged from 0.6-1.17 mL. Additionally, when examining fig. 7, 1.17 mL of water was obtained with the MOF box having a surface area of 0.0619 m², under conditions of 1100 W/m² irradiation, 1.6 m/s air speed, and 200 g of MOF-303 material.

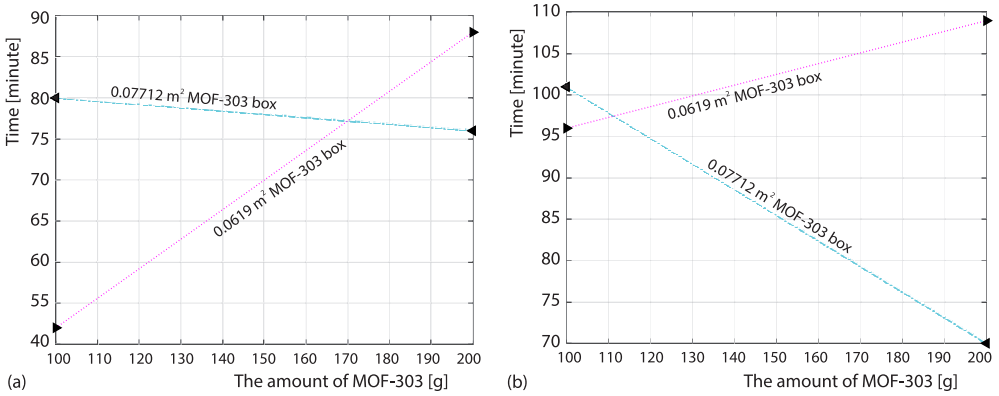

Figure 6. Water production in MOF boxes with different surface areas using different amounts of MOF-303 under 1000 W/m² irradiation; (a) 1.0 m/s air speed and (b) 1.6 m/s air speed

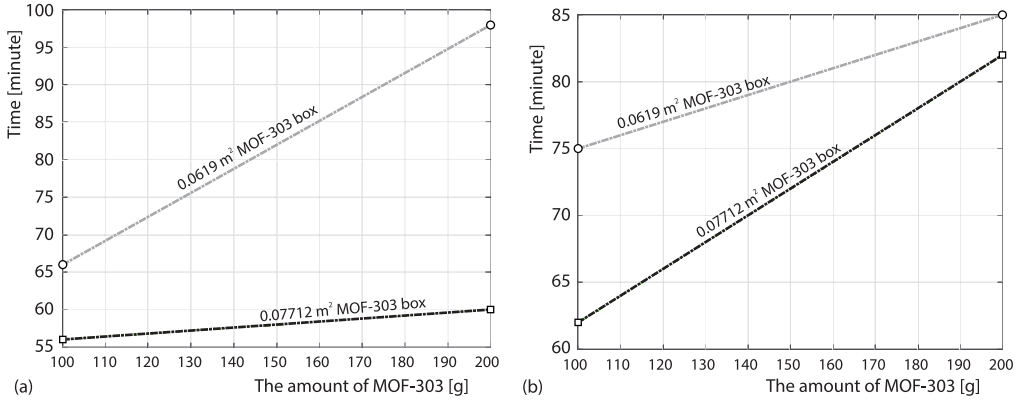

Figure 7. Water production in MOF boxes with different surface areas using different amounts of MOF-303 under 1100 W/m² irradiation; (a) 1.0 m/s air speed and (b) 1.6 m/s air speed

When examining fig. 8, it is observed that the amount of water produced increases with the rise in irradiation intensity and the amount of MOF-303. Studies have demonstrated that the increase in temperature affecting the surface of MOF-303 enhances the material's water release capacity [41]. These findings suggest that an increase in irradiation intensity will also increase the amount of water obtained, and the experimental results align with this expectation.

Additionally, efficiency calculations were performed for three different irradiation levels: 900 W/m^2, 1000 W/m^2, and 1100 W/m^2. The results indicate that as the irradiation intensity increases, the panel surface temperature also rises, leading to a decrease in panel efficiency [38]. This decrease is primarily due to the reduction in output power as the panel surface temperature increases.

The examination of the graphs reveals that for each irradiation level, the thickness of the MOF-303 material increases when its surface area is smaller. The thickness of MOF materials is a critical factor that directly influences adsorption and desorption processes. While a thicker MOF may have a higher capacity to retain water vapor, it also hinders the movement of water vapor within its pores. This leads to an extension of the water production duration. Spe-

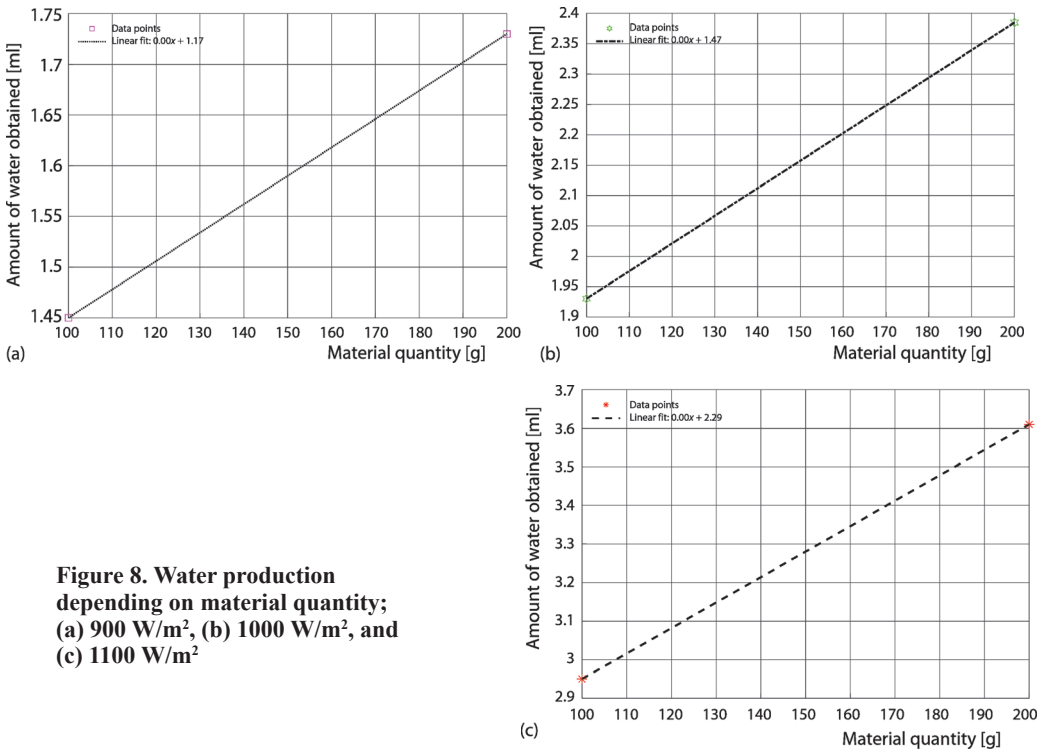

Figure 8. Water production depending on material quantity; (a) 900 W/m², (b) 1000 W/m², and (c) 1100 W/m²

cifically, thicker MOF require water to travel a longer distance to reach the inner layers, which impacts adsorption efficiency and lengthens the water collection process.

Additionally, an increase in air velocity is observed to prolong the water production duration. In cases of high air velocity, the temperature of the air heated by the panel and transferred to the MOF-303 material decreases. This results in a temperature difference between the water vapor in the environment and the MOF. Lower temperatures can negatively affect the MOF's ability to adsorb water vapor, leading to extended water production times [42]. High air velocity causes a temperature drop on the surface of the MOF, slowing down the adsorption process and prolonging the time required to collect water.

In conclusion, the thickness of the MOF-303 material and the air velocity significantly affect water production efficiency. Increased thickness restricts the movement of water molecules, extending the production duration, while high air velocities create a similar effect by causing temperature drops. This highlights the necessity of carefully evaluating parameters such as temperature and thickness when optimizing water production processes. In practical applications, balancing these parameters is critical to enhancing water production efficiency and reducing collection time.

Water production supported by renewable energy using MOF-303 material through PV panels can be considered a significant application in terms of sustainability and environmental protection. In this study, solar energy was utilized both for energy production and to support the water production process, contributing to the reduction of fossil fuel consumption and carbon emissions. This technology alleviates pressure on traditional water resources and supports the preservation of natural ecosystems by enabling water extraction from atmospheric humidity in water-scarce regions. Furthermore, optimizing parameters such as the thickness of MOF-303 ma-

terial, air velocity, and panel temperature reduces energy consumption, minimizes environmental footprints, and enhances material efficiency, making the use of natural resources more sustainable. In the future, large-scale application of materials like MOF-303 will play a critical role in developing resilience against water scarcity and supporting environmental sustainability. Such systems offer a strategic solution mitigate the impacts of global challenges like desertification and climate change. The cooling fans installed beneath PV panels help reduce panel temperatures, preventing energy losses and enhancing system efficiency while minimizing adverse environmental impacts. Additionally, these innovative technologies can significantly contribute to reducing social inequalities and achieving sustainable development goals by facilitating access to energy and water in developing regions. In conclusion, this water production technology supported by MOF-303 material enables more efficient management of energy and water resources, offering a long-term solution for sustainability and environmental protection.

Conclusions

- To evaluate the water production performance of MOF-303 material, the effects of containers with different dimensions were analyzed in detail. Experiments were conducted using two containers with surface areas of 0.0619 m^2 and 0.07712 m^2. The results showed that 6.9 ml of water was obtained from the smaller container, while 7.175 ml of water was collected from the larger container. The reason for the higher water yield in the larger container is its increased exposure to air, as well as the thinner layer of MOF-303, which allows for better pore accessibility and easier condensation.
- In experiments conducted to assess the impact of MOF-303 material on water production, it was observed that increasing the material quantity positively influenced water yield. The results revealed that 6.35 ml of water was obtained with 100 g of MOF-303, whereas 7.725 ml of water was collected with 200 g of the material.
- The air velocity delivered to the surface of the MOF-303 material was tested at two different speeds: 1.0 m/s and 1.6 m/s. The experiments showed that 7.55 ml of water was produced at 1.0 m/s, while 6.525 ml of water was obtained at 1.6 m/s. These findings indicate that higher air velocities have a negative effect on water production due to the decrease in air temperature delivered to the MOF-303 surface as fan speed increases.
- The effect of irradiance intensity on water production was evaluated for three different values: 900 W/m^2, 1000 W/m^2, and 1100 W/m^2. The results showed an increase in water production as irradiance intensity increased. At 900 W/m^2, 3.18 ml of water was collected, while at 1000 W/m^2, the water yield increased to 4.315 ml. At the highest irradiance intensity of 1100 W/m^2, water production reached 6.58 ml. These results demonstrate that increasing irradiance intensity is a significant factor in enhancing water production efficiency, as higher irradiance provides more energy to support the process.
- An application was implemented in which heated air from PV panels was transferred to the surface of MOF-303 for water production. Simultaneously, fan-assisted air-flow was used to cool the panels, minimizing efficiency losses.
- The efficiency of PV panels was evaluated for different irradiance levels. It was found to range between 13.42%-13.61%, 13.29%-13.36%, and 12.85%-12.91% for irradiance levels of 900 W/m^2, 1000 W/m^2, and 1100 W/m^2, respectively.
- Investigations at different irradiance levels showed that the surface temperatures of MOF-303, heated by the hot air delivered, were 51°C, 56°C, and 60°C for 900 W/m^2, 1000 W/m^2, and 1100 W/m^2 irradiance levels, respectively. It was thus concluded that increasing the surface temperature of MOF-303 enhances water production.

Recommendations

- Water obtained using MOF-303 material can be used for irrigation in agriculture.
- The collected water can be utilized for cooling purposes in industrial machinery.
- It can be applied to create water resources in regions with high solar irradiance, such as Chile and Saudi Arabia.
- Water derived from MOF-303 can be used for cooling solar panels and other renewable energy applications.

Acknowledgment

This study was supported by Atatürk University Scientific Research Coordinatorship with number of FDK-2023-13054.

References

[1] Yao, H., *et al*., Highly Efficient Clean Water Production from Contaminated Air with a Wide Humidity Range, *Advanced Materials*, *32* (2020), 1905875
[2] Sivakumar, B., Global Climate Change and Its Impacts on Water Resources Planning and Management: Assessment and Challenges, *Stochastic Environmental Research and Risk Assessment*, *25* (2011), July, pp. 583-600
[3] Hanikel, N., *et al*., Rapid Cycling and Exceptional Yield in a Metal-Organic Framework Water Harvester, *ACS Central Science*, *5* (2019), Aug., pp. 1699-1706
[4] Fathieh, F., *et al*., Practical Water Production from Desert Air, *Science Advances*, *4* (2018), 3198
[5] James, S. L., Metal-Organic Frameworks, *Chemical Society Reviews*, *32* (2003), July, pp. 276-288
[6] Laha, S., Maji, T. K., Binary/Ternary MOF Nanocomposites for Multi-Environment Indoor Atmospheric Water Harvesting, *Advanced Functional Materials*, *32* (2022), 2203093
[7] Sharma, R., *et al*., Ferromagnetic Metal Organic Framework (MOF)/Alginate Hybrid Beads for Atmospheric Water Capture And Induction Heating-Enabled Water Release, *Applied Materials Today*, *35* (2023), 101918
[8] Hanikel, N., *et al*., The MOF Linker Extension Strategy for Enhanced Atmospheric Water Harvesting, *ACS Central Science*, *9* (2023), Mar., pp. 551-557
[9] Luo, F., *et al*., High-Efficient and Scalable Solar-Driven MOF-Based Water Collection Unit: From Module Design to Concrete Implementation, *Chemical Engineering Journal*, *465* (2023), 142891
[10] Bilal, M., *et al*., Adsorption-Based Atmospheric Water Harvesting: A Review of Adsorbents and Systems, *International Communications in Heat and Mass Transfer*, *133* (2022), 105961
[11] Chen, Z., *et al*., Study of the Scale-Up Effect on the Water Sorption Performance of MOF Materials, *ACS Materials Au*, *3* (2022), 1, pp. 43-54
[12] Zheng, Z., *et al*., Broadly Tunable Atmospheric Water Harvesting in Multivariate Metal-Organic Frameworks, *Journal of the American Chemical Society*, *144* (2022), Nov, pp. 22669-22675
[13] Luo, F., *et al*., Bimetallic MOF-Derived Solar-Triggered Monolithic Adsorbent for Enhanced Atmospheric Water Harvesting, *Small*, *19* (2023), 2304477
[14] Almassad, H. A., *et al*., Environmentally Adaptive MOF-Based Device Enables Continuous Self-Optimizing Atmospheric Water Harvesting, *Nature Communications*, *13* (2022), 4873
[15] Wu, J., *et al*., A Study on the Improvement of the Photo-Thermal Characteristics of the Adsorbent for Sorption-Based Atmospheric Water Harvesting Driven by Solar, *Coatings*, *13* (2023), 154
[16] Tao, Y., *et al.*, Electrically Heatable Carbon Scaffold Accommodated Monolithic Metal-Organic Frameworks for Energy-Efficient Atmospheric Water Harvesting, *Chemical Engineering Journal*, *451* (2023), 138547
[17] Li, A., *et al.*, A Rapid-Ab/Desorption and Portable Photo-Thermal MIL-101(Cr) Nanofibrous Composite Membrane Fabricated by Spray-Electrospinning for Atmosphere Water Harvesting, *Energy & Environmental Materials*, *6* (2023), e12254
[18] Logan, M. W., *et al*., Reversible Atmospheric Water Harvesting Using Metal-Organic Frameworks, *Scientific Reports*, *10* (2020), 1492
[19] Fuchs, A., *et al*., Water Harvesting at the Single-Crystal Level, *Journal of the American Chemical Society*, *145* (2023), June, pp. 14324-14334

[20] An, H., *et al*., High-Performance Solar-Driven Water Harvesting from Air with a Cheap and Scalable Hygroscopic Salt Modified Metal-Organic Framework, *Chemical Engineering Journal*, *461* (2023), 141955
[21] Wu, Q., *et al*., Spray-Applied MXene Coatings on Metal-Organic Framework Monoliths for Adaptive All-Day Atmospheric Water Harvesting at Mitigated Energy Cost, *Industrial & Engineering Chemistry Research*, *63* (2024), Mar., pp. 4866-4875
[22] Suh, B. L., *et al*., Photochemically Induced Water Harvesting in Metal-Organic Framework, *ACS Sustainable Chemistry & Engineering*, *7* (2019), Sept., pp. 15854-15859
[23] Tao, Y., *et al*., Tubular Metal-Organic Framework Membranes Enabling Exceptional Atmospheric Water Harvesting by Fast Air Permeation, *Chemical Engineering Journal*, *461* (2023), 141864
[24] Deng, F., *et al*., The 3-D Conical Absorbent Design for Enhancing Atmospheric Water Harvesting Performance, *Chinese Science Bulletin*, *67* (2022), Feb., pp. 906-912
[25] Liu, X., *et al*., Metal-Organic-Framework-Based Polymers for Effective Water Harvesting in Arid Areas, *ACS Applied Polymer Materials*, *5* (2023), Oct., pp. 9159-9169
[26] Jimenez-Laines, G., *et al*., Double Step Heating Synthesis of MIL-101 (Cr) Composites For Water Harvesting Applications, *Microporous and Mesoporous Materials*, *362* (2023), 112782
[27] Kim, H., *et al*., Water Harvesting from Air with Metal-Organic Frameworks Powered by Natural Sunlight, *Science*, *356* (2017), Apr., pp. 430-434
[28] Terzis, A., *et al*., High-Frequency Water Vapor Sorption Cycling Using Fluidization of Metal-Organic Frameworks, *Cell Reports Physical Science*, *1* (2020), 100057
[29] Kim, H., *et al.*, Adsorption-Based Atmospheric Water Harvesting Device for Arid Climates, *Nature Communications*, *9* (2018), 1191
[30] VanLeuven, C. C., *et al*., Water Harvesting Properties of a Zwitterionic Metal-Organic Framework, *Molecular Systems Design & Engineering*, *8* (2023), Mar., pp. 580-585
[31] Hanikel, N., *et al*., Evolution of Water Structures in Metal-Organic Frameworks for Improved Atmospheric Water Harvesting, *Science*, *374* (2021), Oct., pp. 454-459
[32] An, L., *et al.*, Liquid Metal Nanolayer-Linked MOF Nanocomposites by Laser Shock Evaporation, *Matter*, *4* (2021), Dec., pp. 3977-3990
[33] Feng, Y., *et al*., Active MOF Water Harvester with Extraordinary Productivity Enabled by Cooling-Enhanced Sorption, *Energy & Environmental Science*, *17* (2024), Dec., pp. 1083-1094
[34] Shen, Q., *et al*., Novel Pyrazole-Based MOF Synergistic Polymer of Intrinsic Microporosity Membranes for High-Efficient CO_2 Capture, *Journal of Membrane Science*, *664* (2022), 121107
[35] Torres-Herrera, U., *et al.*, Water Harvesting by Molecular Sieves Using Self-Sustained Continuous Flow, *Transport in Porous Media*, *149* (2023), June, pp. 479-499
[36] Kim, H., *et al*., Thermodynamic Analysis and Optimization of Adsorption-Based Atmospheric Water Harvesting, *International Journal of Heat and Mass Transfer*, *161* (2020), 120253
[37] Lassitter, T., *et al*., Mass Transfer in Atmospheric Water Harvesting Systems, *Chemical Engineering Science*, *285* (2024), 119430
[38] Guven, S., Investigation of the Effect of Photovoltaic Panel Surface Temperature on Output Power and Efficiency for Denizli Province (in Turkish), *Mühendis ve Makina*, *63* (2022), June, pp. 429-442
[39] Elsayed, E., *et al*., The MOF Based Coated Adsorption System for Water Desalination and Cooling Integrated with Pre-Treatment Unit, *Sustainable Energy Technologies and Assessments*, *56* (2023), 103006
[40] Cheng, L., *et al.*, Recent Advances in Metal-Organic Frameworks for Water Absorption and Their Applications, *Materials Chemistry Frontiers*, *8* (2024), Nov., pp. 1171-1194
[41] Alkhatib N., *et al.*, How does MOF-303 Achieve High Water Uptake And Facile Release Capacity, *The Journal of Physical Chemistry C*, *128* (2024), May, pp. 8384-8394
[42] Liu, S., *et al*., Characterization of Water Vapor Sorption Performance and Heat Storage of MIL-101 (Cr) Complex $MgCl_2$, $LiCl/LaCl_3$ System For Adsorptive Thermal Conversion, *ACS Omega*, *9* (2023), Dec., pp. 509-519

Paper submitted: March 15, 2025
Paper revised: June 18, 2025
Paper accepted: July 23, 2025